Modelling the effects of climate change on the distribution and production of marine fishes: accounting for trophic interactions in a dynamic bioclimate envelope model

Jose A. Fernandes[1,2,*], William W. L. Cheung[3], Simon Jennings[1,4], Momme Butenschön[2], Lee de Mora[2], Thomas L. Frölicher[5], Manuel Barange[2], Alastair Grant[1]

[1] School of Environmental Sciences, The University of East Anglia, Norwich, UK
[2] Plymouth Marine Laboratory, Prospect Place, The Hoe, Plymouth, UK
[3] Changing Ocean Research Unit, The University of British Columbia, Vancouver, BC, Canada
[4] Centre for Environment, Fisheries and Aquaculture Science, Lowestoft, UK
[5] Atmospheric and Oceanic Sciences Program, Princeton University, Princeton, NJ, USA

*: Corresponding author : Jose A. Fernandes, tel. +44 (0)1603591375 ; fax +44 (0)1752633101 ;
email address : j.fernandes@uea.ac.uk

Abstract:

Climate change has already altered the distribution of marine fishes. Future predictions of fish distributions and catches based on bioclimate envelope models are available, but to date they have not considered interspecific interactions. We address this by combining the species-based Dynamic Bioclimate Envelope Model (DBEM) with a size-based trophic model. The new approach provides spatially and temporally resolved predictions of changes in species' size, abundance and catch potential that account for the effects of ecological interactions. Predicted latitudinal shifts are, on average, reduced by 20% when species interactions are incorporated, compared to DBEM predictions, with pelagic species showing the greatest reductions. Goodness-of-fit of biomass data from fish stock assessments in the North Atlantic between 1991 and 2003 is improved slightly by including species interactions. The differences between predictions from the two models may be relatively modest because, at the North Atlantic basin scale, (i) predators and competitors may respond to climate change together; (ii) existing parameterization of the DBEM might implicitly incorporate trophic interactions; and/or (iii) trophic interactions might not be the main driver of responses to climate. Future analyses using ecologically explicit models and data will improve understanding of the effects of inter-specific interactions on responses to climate change, and better inform managers about plausible ecological and fishery consequences of a changing environment.

Keywords: biological feedback ; climate change ; competition ; ecosystem approach ; fisheries management ; model validation ; modelling ; size spectrum ; species interactions

Introduction

Climate change affects ocean conditions, including temperature, salinity, ice coverage, currents, oxygen level, acidity, and consequently growth, body size, distribution, productivity and abundance of marine species, including those that are exploited by fisheries (Behrenfeld *et al.* 2006; Brander 2007; Perry *et al.* 2005; Pörtner 2010; Simpson *et al.* 2011, Cheung *et al.* 2013). Over a range of greenhouse gas emission scenarios (IPCC 2007), changes in the marine environment are predicted to be more rapid in the 21st century with implications for marine ecosystems and dependent industries (Roessig *et al.* 2004; Lam *et al.* 2012; Merino *et al.* 2012).

A range of modelling approaches has been developed to predict the potential effects of future climate change on species distributions and abundance (Stock *et al.* 2011). One class of models, species-based bioclimate envelope models, have been used to predict redistribution of both terrestrial and aquatic species (Pearson and Dawson 2003; Jones *et al.* 2012). The Dynamic Bioclimate Envelope Model (DBEM) developed by Cheung *et al.* (2008a, 2008b, 2009, 2011) projects changes in marine species distribution, abundance and body size with explicit consideration of population dynamics, dispersal (larval and adult) and ecophysiology (Cheung *et al.* 2008a, 2008b, 2009, 2011, 2013). Projections suggest that there will be a high rate of species invasions in high-latitude regions and a potential high rate of local extinction in the tropics and semi-enclosed seas in the 21st century (Cheung *et al.* 2009). Moreover, as a result of predicted changes in range and primary productivity, Cheung *et al.* (2010) project that maximum catch potential of exploited species is expected to decrease in the tropics and to increase in high latitudes. However, these projections do not account for the effects of species interactions on redistribution and abundance, thus introducing a source of structural uncertainty (Cheung *et al.* 2010).

Rates of primary production and transfer efficiency influence production and biomass of consumers. 'Size-spectrum' models have been developed to describe energy transfer from primary producers to consumers of progressively larger body size (e.g. Dickie *et al.* 1987) and variants of these models have been developed and applied to predict potential biomass, production and size structure of fish in the world's oceans from estimates of primary production and temperature (Jennings *et al.* 2008), and to predict the responses of fish communities to fishing and climate change (Blanchard *et al.* 2011, 2012). These size-based models are not taxonomically resolved, and this limits the range of applications, given that species identity is usually a key consideration for management, monitoring and regulatory purposes.

Here, we combine the strengths of the DBEM (i.e., focus on identified species) with those of the size spectrum model (i.e., focus on trophic interactions) to predict spatial and temporal changes in species' abundance and distribution in response to predicted future changes in temperature and primary production. Forty-eight of the most abundant and commercially important marine fishes in the North Atlantic, here defined as Food and Agriculture Organization (FAO) statistical area 27, are included. The size spectrum is used to determine resource limits in a given geographical area and these limits, along with habitat suitability for a given species, determine the biomass of that species that can be supported in this area.

Materials and methods

A modelling approach that integrates the species-based DBEM model with the size spectrum approach, hereafter called size-spectrum DBEM (SS-DBEM) was developed. The SS-DBEM: (1) estimates potential biomass supported by the system, (2) predicts habitat suitability and (3) models species interactions. Predictions from the SS-DBEM are then compared with those from a DBEM model that does not incorporate species interactions (NSI-DBEM, where NSI denotes no species interactions).

Potential biomass supported at each body size class

The size-spectrum is described as a log-log relationship between abundance and body size. The slope of the spectrum is determined by trophic transfer efficiency and the relationships between the body sizes of predators and their prey (Borgmann 1987; Jennings and Mackinson 2003). The height of the spectrum is determined by primary production and describes the total abundance of individuals from all species that can be supported in any defined body size class (e.g. Boudreau and Dickie 1992).

Since predator-prey mass ratios and transfer efficiencies in marine food chains do not depend systematically on the mean rate of primary production or mean temperature (Barnes *et al.* 2010), less energy is transferred to consumers of a given body size when food webs are supported by smaller primary producers (Barnes *et al.* 2010). Much of the variation in the body size distribution of primary producers depends on the absolute rate of primary production, with picoplankton, the smallest phytoplankton, dominating when primary production is low (Agawin *et al.* 2000). Thus the median and mean body sizes of phytoplankton decrease with decreasing rates of primary production (Barnes *et al.* 2011). To account for this, the position of the median body mass class for phytoplankton (m) was calculated as:

$$m = [(-6.1 \cdot P_s) - 8.25]/\log_{10}(2) \tag{1}$$

where P_s is the predicted contribution of picophytoplankton net production to total net Primary Production (PP) as calculated using the empirical equation

$$P_s = [(12.19 \log PP) + 37.248]/100 \tag{2}$$

derived by Jennings *et al.* (2008) using the data from Agawin *et al.* (2000).

Once the median body mass class of phytoplankton was defined, we calculated the consumer biomass at body size following the approach of Jennings *et al.* (2008). Assumptions about trophic transfer efficiency and the predator-prey mass ratio ($\varepsilon = 0.125$ and $\mu = 3$, respectively) followed Jennings *et al.* (2008), but the spectrum was discretized using a $\log_2$ series of body mass from 2^{-1} to 2^{19} g. Subsequent evidence suggests that the predator-prey mass ratio may increase with body mass and that transfer efficiency may decrease, but the changes are not expected to affect the time-averaged slope of the size-spectrum (Barnes *et al.* 2010).

Habitat suitability

The prediction of habitat suitability in SS-DBEM was based on the algorithm implemented in NSI-DBEM (Cheung *et al.* 2008a, 2008b, 2009, 2011, 2012). The NSI-DBEM defines the

relative preferences of the modelled species for temperature and other environmental variables based on the relationship between current distributions and gridded environmental data. The initial distribution of relative abundance (representing 1970 – 2000) of the modelled marine species on a 30' x 30' latitude-longitude grid map of the world ocean are predicted using the *Sea Around Us* project algorithm (Close *et al*. 2006; Jones *et al.* 2012) based on parameters describing range limits, association with major habitat types and known occurrence boundaries. Parameter values for each species were derived from data in online databases, mainly FishBase (www.fishbase.org) and SeaLifeBase (www.sealifebase.org). Environmental variables incorporated into the NSI-DBEM include sea surface temperature, sea bottom temperature, coastal upwelling, salinity, sea-ice extent, depth and habitat types (Cheung *et al.* 2011). NSI-DBEM first calculates changes in growth and other life history traits in response to changes in temperature and oxygen concentration based on algorithms derived from growth and metabolic functions and empirical equations (Cheung *et al*. 2011, 2013). Second, NSI-DBEM predicts size-frequency distributions for each species in each spatial cell using a size-structured 'per recruit' model. Finally, the model simulates spatial and temporal changes in relative abundance within a cell based on carrying capacity of a cell, density-dependent population growth, larval dispersal and adult migration (Cheung *et al.* 2008b, 2011).

Species interactions

A new algorithm was developed to describe resource competition between different species co-occurring in a cell by comparing the energy (in biomass) that can be supported in the cell (estimated with the SS model) with the energy demanded by the species predicted to inhabit the given cell (estimated with the NSI model). The algorithm comprises two stages: (1) an initialization stage where competition parameters are estimated; and, (2) a recurrent stage where the competition parameters are used to resolve conflicts between energy (biomass) demands and biomass that can be supported. One advantage of this approach is that it focuses on competition for the energy available within a cell, thus negating the need for a diet matrix that describes species-specific feeding interactions. Data to develop such matrices are scarce at the scale of FAO Area 27 and the persistence and emergence of feeding interactions through time, and in response to future climate change, is highly uncertain.

First stage

The model uses the NSI-DBEM approach to establish an initial distribution for each species. The approach assumes that predicted habitat suitability is a proxy for the distribution of relative abundance of a given species. Thus, multiplying the initial relative biomass by the estimated absolute biomass from empirical data, initial species distribution is expressed in terms of absolute biomass in each cell. Since biomass estimates from assessment data are not available for some of the species considered (Table 1), the initial biomass estimates were approximated by the predicted unexploited biomass (B_∞) from maximum reported fisheries catch (MC) since 1950 and an estimate of the intrinsic growth rate (*r*) of the population (Schaefer 1954):

$$B_\infty = MSY \cdot 4/r \tag{3}$$

Maximum sustainable yield (MSY) was calculated using the algorithm documented in Cheung *et al*. (2008) that used the average maximum value of the catch time-series of a species as an approximated MSY. Values for *r*, estimated based on an empirical equation that was dependent on asymptotic length of the species, were obtained from FishBase (www.fishbase.org). Although this is an approximation and not as reliable as estimates of

biomass using survey-based methods (Pauly *et al.* 2013), we show that, consistent with similar findings by Froese *et al.* (2012), that biomass estimates from maximum catch data were significantly correlated with those from aggregated stock assessments (Table 1, Fig. 1). These biomass estimates were used for model initialization only.

The initial absolute biomass estimates, based on habitat suitability in the cells where they are distributed (Fig. 2), are used to generate a matrix of species' energy demand (expressed as biomass). Matrix elements define the proportion of total energy obtained by a species at each habitat suitability bin and size class. The amount of energy is determined by the average proportion of energy that a species gets in cells with the same habitat suitability.

Energy demanded (E_D) by a species in a cell is compared with the total biomass or energy (E_S) that can be supported in the cell (see Table 2 for a summary of abbreviations). E_D is determined based on the predicted habitat suitability from the DBEM algorithm, whereas E_S is determined by the SS model. Thus, the average proportion of energy that a species demands in cells with the same habitat suitability can be calculated:

$$resouces_{Spp,Suit,Size} = \frac{E\_D_{Spp,W,i}^{Suit}}{E\_S_{W,i}} \tag{4}$$

To convert from biomass (B) distribution to numbers (N) and *vice versa*, the mean body mass (W) at each size class (*i*) is used:

$$B = \sum_{i=1}^{n} N_i \times W_i \tag{5}$$

where n is the number of size classes considered in the model. The initial habitat suitability value is converted using a square root data transformation, to ensure a balanced distribution of the cells across the habitat suitability classes, and then normalized to a range from 0 to 1 relative to minimum and maximum value of habitat suitability for each species. The model then groups habitat suitability into six classes (bins) of values: 0 - 0.3, >0.3 - 0.4, >0.4 - 0.5, >0.5 - 0.6, >0.6 - 0.7 and >0.7 - 1. The use of discretized bins of habitat suitability, a non-parametric methodology, does not require the specification of explicit distribution functions and is more computationally efficient (Fayyad and Irani 1993; Dougherty *et al.* 1995). The effects of such discretization are minimized here by square root transformation of the predicted habitat suitability, the low number of bins and the choice of bin boundaries (Uusitalo 2007; Fernandes *et al.* 2010).

Available energy in a size class which is not demanded by the modelled species was assigned to a group called '*Other groups*', because species that were not modelled explicitly would also have an energy demand. This group has its own resource allocation matrix based on the average habitat suitability of the modelled species, allowing the inclusion of resource demand from species that are not explicitly modelled. Since the species assemblage in the boundary of the geographic domain of the model is likely to be under-represented by the modelled species, the matrix for '*Others* group' is only computed for cells where the number of species present is more than the square root of the total number of species modelled.

Second stage

Abundance of each species in each cell was predicted using the algorithm in the NSI-DBEM. The model runs uses an annual time-step for bottom-dwelling (demersal) species and two seasonal time-steps (summer and winter) for species in the water-column (pelagic). The energy demand of each species is compared with energy demands of other species co-

occurring in the same cell (Fig. 2). If the energy demanded by all organisms in the cell exceeds the energy available, then the available energy is allocated to each species in proportion to its energy demands. If the energy demanded by all the species is lower than the energy available, the surplus energy is allocated according to the proportional energy demand of the species present, including the '*Others group*'. To represent population growth that is limited by factors other than available energy, the rate at which energy can be assimilated by a species is limited:

$$\text{res\_op}_{\text{Spp,Suit,W}} = \frac{2 \cdot \text{std.dev}(\text{E\_D}^{\text{Suit}})}{\text{mean}(\text{E\_D}^{\text{Suit}})} \tag{6}$$

where, E_D^{Suit} denotes the energy demanded in all the cells in each bin of habitat suitability. Therefore, the amount of additional energy that can be taken by the species is limited by two times the standard deviation (std.dev) of energy that each species gets in the initial distribution to each habitat suitability bin. Any energy that is left after these allocations is assumed to be used by the '*Others group*'.

Model testing

The results from the model that includes competition were compared with results from the NSI-DBEM and "empirical" time series of abundance data from fish stock assessments for the Northeast Atlantic (FAO area 27), as extracted from the RAM Legacy Stock Assessment Database (Ricard *et al.* 2011; http://ramlegacy.marinebiodiversity.ca/) and ICES Stock Summary Database (http://www.ices.dk). To compare projected changes with observations, abundance data for each species were normalized by dividing them by their mean value. While the models were applied to a set of 48 fish species, comparison with empirical data was conducted for 24 species for which data were available from the RAM Legacy and ICES databases (Table 1). The output of the DBEM models were compared with the "empirical" time series values for each species and distribution of absolute error (AE) was calculated:

$$\text{AE} = \left| p_j - x_j \right| \tag{7}$$

where p is the total biomass predicted in a DBEM model in a particular year for a species j, and x is the total biomass from the assessments. The comparison was done for the years with available assessment data for all the 24 species considered (1991-2003). To compare the performance of the SS-DBEM and NSI-DBEM, the Percent Reduction in Error (PRE) was calculated (Hagle and Glen 1992; Fernandes *et al.* 2009), but weighted by the maximum catch of each species (WPRE):

$$\text{WPRE} = \frac{1}{\sum_{k=1}^{l} \text{MaxCatch}_k} \sum_{k=1}^{l} \left[\frac{100(\text{AENSI}_k - \text{AESS}_k)}{\text{AENSI}_k} \right] \cdot \text{MaxCatch}_k \tag{8}$$

where AENSI is the absolute error in the NSI-DBEM model, AESS is the absolute error in the SS-DBEM model, k the number of species and MaxCatch the maximum catch of the species.

These models were also compared with empirical data describing latitudinal and depth centroid shifts of species in response to climate change (Dulvy *et al.* 2008; Cheung *et al.* 2011). Distribution centroid (DC_t) for each year (t) was calculated as:

$$DC_t = \frac{\sum_i^n B_{t,i} \cdot A_i \cdot Lat_i}{\sum_i^n B_{t,i} \cdot A_i}; \qquad (9)$$

where, B_i is the predicted relative abundance in cell i, A is the area of the cell, Lat is the latitude at the centre of the cell and n is the total number of cells where the species was predicted to occur. We calculated the rate of range shift as the slope of a fitted linear regression between the distribution centroid of the species and time. We expressed latitudinal range shift (LS) as poleward shift in distance from:

$$LS = DS \cdot \pi / 180 \cdot 6378.2; \qquad (10)$$

where DS is the distribution shift in degree latitude per year.

The models were run for 35 years, from 1970 to 2004, with environmental forcing predicted from two modelling systems: (1) the National Oceanographic and Atmospheric Administration (NOAA) Geophysical Fluid Dynamic Laboratory Earth System Model (ESM) 2.1 (GFDL) and (2) the European Regional Seas Ecosystem Model (ERSEM). GFDL ESM2.1 is a global atmosphere-ocean general circulation model (Delworth *et al*. 2006) coupled to a marine biogeochemistry model (TOPAZ; Dunne *et al.* 2010) which includes major nutrients and three phytoplankton functional groups with variable stoichiometry. For the GFDL hindcast simulations (Henson *et al.* 2010), air temperature and incoming fluxes of wind stress, freshwater, shortwave and longwave radiation are prescribed as boundary conditions from the CORE- version 2 reanalysis effort (Large and Yeager 2009). ERSEM is a biogeochemical model that uses a functional-groups approach incorporating four phytoplankton and three zooplankton functional groups and decouples carbon and nutrient dynamics (Blackford *et al.* 2004). Data from two different configurations of ERSEM were applied here: on the global scale a hindcast of the NEMO-ERSEM model forced with DFS 4.1 reanalysis for the atmosphere (Dunne *et al*. 2010) and on the regional scale a hindcast of the POLCOMS-ERSEM model for the NW-European shelf forced with ERA 40 reanalysis (extended with operational ECMWF reanalysis until 2004) for the atmosphere and global ocean reanalysis for the open ocean boundaries (more details on the configuration can be found in Holt *et al.* 2012; Artioli *et al.* 2012). The domain of this global model overlapped the domain of a regional model of the North Sea area.

Results and discussion

Performance of SS-DBEM and NSI-DBEM

Predicted biomasses from SS-DBEM were generally lower than those projected from NSI-DBEM (Fig. 3). The reason is that the energy available from primary producers limits species' biomass in SS-DBEM but not in NSI-DBEM, where species' carrying capacity depends mainly on the habitat suitability of the cell. The algorithm in SS-DBEM explicitly modelled interspecific competition for energy, based on size considerations, without specifying these interactions (e.g. no diet matrix). Our approach allows for the development of scenarios of large-scale shift in species distribution and catches, complementing other models that have been designed to achieve this (Cheung *et al.* 2010; Metcalfe *et al.* 2012).

Outputs from SS-DBEM explain slightly more of the variation in biomass estimated from stock assessments (FAO area 27) than those from the NSI-DBEM. The error weighted by maximum catch predicted across species from SS-DBEM against empirical data is 3.7% lower than those predicted from NSI-DBEM using GFDL environmental forcing data and 0.6% lower using ERSEM data. GFDL might be more accurate (Fig. 4) for the time period considered since the model run was forced by re-analysis data such as surface temperature and wind fields, which is not the case for ERSEM. However, the differences in mean absolute error are not significant and might not hold when the models are used for forecasting. Future work will explore the causes of this difference, which may not depend on the modelling itself but on input data such as environmental forcing, or even on the adequacy of the assessment data used for the comparison. Finally, a lower variance in the absolute error in SS-DBEM with respect to NSI-DBEM model (Fig. 4) is indicative of a higher precision of simulated biomass from SS-DBEM (Taylor 1999). This also supports the view that the proposed modelling approach is a potential advance over models that do not account for species interactions.

Distribution shifts

Both NSI-DBEM and SS-DBEM projected poleward latitudinal shift of species distributions (Fig. 5), and the projected shifts are generally consistent between simulations forced by the two sets of Earth System Model outputs (Table 3). In addition, the projected shift of pelagic species by the model with interactions is consistently lower than if no interactions are considered (Table 3). With ERSEM forcing, the median projected rates of poleward shift are 63.5 km and 54.9 km over 35 years, or 18.1 and 15.7 km decade^{-1}, from NSI-DBEM and SS-DBEM respectively. Similar to previous analysis using NSI-DBEM, all sets of simulations show a higher rate of range shift for pelagic species than bottom dwelling species (Cheung *et al*. 2009, Jones *et al*. 2013). A reduction in the expected geographical shift of particular populations as a result of ecological interactions is consistent with the perception of compensatory ecological processes (Frank *et al.* 2011). Shifts in depth are also observed and are strongly driven by the forcing model considered. The shift in depth is also dependent on the spatial domain considered. For example, for demersal species in FAO Area 27, outputs from SS-DBEM driven by ERSEM data project a shift to deeper waters of 1.3 m decade^{-1}. However, when we consider North Sea only, the projected shift to deeper waters is higher at 5.7 m decade^{-1}.

The slower rates of projected shifts from the SS-DBEM relative to NSI-DBEM are consistent with previous literature based on recent observations. Specifically, Perry *et al.* (2005) projected a mean rate of latitudinal shift of 22 km decade[-1] from 1980 to 2004 in the North Sea for six fish species. Comparable rates of shift (between 18.5 and 18.8 km decade[-1]) are projected here for our modelled subset of species which includes four of these species (bib, blue whiting, Norway pout and witch). Also, Dulvy *et al.* (2008) estimated that bottom dwelling species were moving into deeper waters at an average rate of 3.1 m decade[-1] from 1980 to 2004 (19 species out of 28 species are common between this study and Dulvy *et al.* 2008), which is slower than our prediction of 5.7 m decade[-1]. These direct comparisons between predicted and observed shifts need to be interpreted with caution because of differences in the species included, the spatial domains, and the time period considered. In addition, our simulations represent average species-level changes without consideration for stock structure, owing to incomplete biological data to address the latter. The trend in abundance or range shift of a given species may not necessarily be equivalent to that of every stock of that species (Petitgas *et al.* 2012).

Maximum catch
The maximum catch predicted by both DBEM models (SS and NSI) broadly follows multi-decadal variability in empirical estimates of total catches for the 1970 to 2004 time period in the ICES areas (Fig. 6). This is demonstrated by maximum and minimum points in similar years, with the highest discrepancy in years around 1985. All the time series show higher maximum values in the first half of the time period and consistently lower maximum values in the second half. However, this negative trend in catches in all the time-series is not statistically significant. The empirical catch data are aggregated catches by all species reported in ICES areas as collected in the Eurostat/ICES database on catch statistics (http://www.ices.dk). The predicted maximum catch is based on the aggregation of the potential catch of the 48 modelled species in ICES areas. Despite some discrepancies, the models are able to reproduce general trends in observed fisheries productivity in the North East Atlantic, providing some confidence in their utility.

Catches predicted from SS and NSI approaches show similar patterns when the most abundant and commercially important species are aggregated. Further work will focus on examining the effects of different modelling approaches on catch predicted for specific species, areas (e.g. ICES areas) or size classes.

Model uncertainty
Projections from NSI- and SS-DBEM are sensitive to the environmental variables projected by the Earth System Models and used to force the ecological models. Earth System Models have a number of limitations when applied to fisheries problems (Stock et al. 2011). Their resolution is relatively coarse to capture ecological processes (generally ~1 degree in the ocean) and they also do not capture well the coastal and continental shelf ocean dynamics. As a result, Earth System Models are known to systematically project lower primary production in coastal areas (Steinacher et al. 2010). Inter-model spread arises from diverse sources, such as the parameters chosen for sub-grid-scale parametrizations. In addition, there is overall limited availability of reliable data to calibrate the models. Efforts to improve the understanding and projections for primary production are ongoing (e.g. Holt et al. 2012, Krause-Jensen et al. 2012), which will likely contribute to improved performance of DBEM models.

An assumption of the size-spectrum component of the model is the linear relationship between log-abundance and log-body size classes in the cell. Such an assumption is made mainly for computational performance. In reality, it may be violated by species' migrations that lead to energy losses and subsidies from given cells, and by seasonal fluctuations in primary production (Blanchard *et al.*, 2010).

The relative abundance of individuals at size can be modified by the overall constraints on energy availability. In general, these have limited effect on the projections because the changes account for a small percentage of the total abundance of species in the cell (an average of 0.03 % of abundance decrease). However, the absolute effects are larger and occur in more cells for whiting, blue whiting, Atlantic cod, Norway pout, European plaice, saithe and Atlantic horse mackerel.

The DBEM modelling approaches have a number of inherent assumptions and uncertainties that may affect the performance of the models (Cheung *et al.* 2009). First, the models are based on the assumption that the predicted current species distributions depict the environmental preferences of the species and are in equilibrium. Second, the underlying biological hypothesis, represented by the model structure and input parameters, may be uncertain. Moreover, the models did not consider the potential for phenotypic and evolutionary adaptations of the species. Since these assumptions apply to both NSI- and SS-DBEM, they do not affect the comparison of projections between the two models. We used theory and empirical data to model trophic interactions. The modelling approach does not incorporate the full range or complexity of interactions among species. This simplification avoids the difficulties of formalising transient and complex species-specific predatory interactions at large-scales. It also requires no assumptions about the extent to which species-specific trophic interactions that are seen today will persist in the future. Furthermore, at the system level, size-based processes account for much of the variation in prey choice and trophic structure.

Survey data can provide an alternative way of validating model outputs (Simpson *et al.* 2011). However, there are scale reasons why we did not pursue this type of validation in this study. Fisheries surveys tend to focus on particular species assemblages (e.g. pelagic or bottom-dwelling species), and are designed to provide a geographical and temporal snapshot that fits with the life history of target species. As such they are not very comparable to model outputs for a large geographical area (FAO area 27).

There are small but quantifiable improvements in goodness-of-fit with stock assessment abundance estimates, predictions of latitudinal shifts and comparisons with predicted maximum catch and observed catches. However, we need to be cautious about our interpretations of model performance at this stage owing to structural and parameter uncertainties, and uncertainties in the models used to generate the environmental forcing. The similarity of predictions might reflect incorrect assumptions. For example, we assume that single species models do not account for species interaction because there is no explicit mechanism, even though species interactions might already be implicitly incorporated in its parameterization (e.g. habitat suitability calculation from observed distribution data). The similarity of predictions might also be attributed to the similar effects of changing climate on many predators and competitors and the implicit assumption of the NSI-DBEM approach that the importance of inter-specific interactions remains the same. In addition, trophic interactions might not be the main driver of responses to climate at the basin scale. Therefore, our results at the scale of the North Atlantic basin, or aggregated ICES areas, does not mean that trophic interactions may not have more influence on regional and local responses.

Unfortunately, the earth system and ecological models described in this paper are too complicated to allow comprehensive explorations of the effects of changing model structures and parameterisation. Such explorations could be achieved in the long-term by comparing projections from the DBEMs with alternative parameter settings for larger datasets of time-series of changes in distribution and abundance from different ocean regions.

The main benefit of our model comes from unifying two modelling approaches providing spatially and temporally resolved species and size predictions, with full consideration for the effects of ecological interactions. Future development of the DBEM will also attempt to incorporate other key biological processes that are likely to be important in determining the responses of marine fishes and invertebrates to climate change. Our model has provided new insight into the effects of ecological interactions on responses to climate and provides a new tool for further exploring the effects of future climate change. Predictions, in conjunction with those from other models, will inform managers about the range of possible ecological and fishery responses to a changing environment, thus supporting the development of management systems that take account of the effects climate change (Perry *et al* 2011) and the on-going implementation of an ecosystem approach to fisheries (Garcia and Cochrane 2005; Rice 2011). Predictions of the long-term effects of climate currently need to be considered alongside those used for operational management, to prepare policy makers and fisheries governance systems for changes in target fisheries and dependent communities and economies (Perry *et al.* 2011).

Acknowledgements

References

Agawin NSR, Duarte CM, Agust S. (2000) Nutrient and temperature control of the contribution of picoplankton to phytoplankton biomass and production. *Limnology Oceanography* 45, 591–600.

Artioli Y, Blackford JC, Butenschön M, *et al.* (2012) The carbonate system in the North Sea: Sensitivity and model validation. *Journal of Marine Systems* 102-104, 1-13.

Barnes C, Maxwell D, Reuman DC, Jennings S. (2010) Global patterns in predator-prey size relationships reveal size dependency of trophic transfer efficiency. *Ecology* 91 (1), 222-232.

Barnes C, Irigoien X, De Oliveira JA, Maxwell D, Jennings S (2011) Predicting marine phytoplankton community size structure from empirical relationships with remotely sensed variables. *Journal of Plankton Research* 33 (1), 13-24.

Behrenfeld MJ, O'Malley RT, Siegel DA, McClain CR, Sarmiento JL, Feldman GC, Milligan AJ, Falkowski PG, Letelier RM, Boss ES (2006) Climate-driven trends in contemporary ocean productivity. *Nature* 444, 752-755.

Blackford JC, Allen JI, Gilbert FJ (2004) Ecosystem dynamics at six contrasting sites: a generic modelling study. *Journal of Marine Systems* 52 (1), 191-215.

Blanchard JL, Law R, Castle MD, Jennings S (2011) Coupled energy pathways and the resilience of size-structured food webs. *Theoretical Ecology* 4 (3), 1-12.

Blanchard JL, Jennings S, Holmes R, Harle J, Merino G, Allen I, Holt J, Dulvy NK, Barange, M (2012) Potential consequences of climate change for primary production and fish production in large marine ecosystems. *Philosophical Transactions of the Royal Society* B, 367, 2979-2989.

Borgmann, U (1987) Models of the slope of, and biomass flow up, the biomass size spectrum. *Canadian Journal of Fisheries and Aquatic Sciences*, 44 (Supplement 2), 136-140.

Boudreau PR, Dickie LM (1992) Biomass spectra of aquatic ecosystems in relation to fisheries yield. *Canadian Journal of Fisheries and Aquatic Science*, 49, 1528-1538.

Brander KM (2007) Global fish production and climate change. *Proceedings of the National Academy of Sciences* 104 (50), 19709-19714.

Cheung WWL, Close C, Lam V, Watson R, Pauly D (2008a) Application of macroecological theory to predict effects on climate change on global fisheries potential. *Marine Ecology Progress Series* 365, 187-197.

Cheung WWL, Lam VWY, Pauly D (2008b) Modelling Present and Climate-Shifted Distribution of Marine Fishes and Invertebrates. Fisheries Centre Research Report 16(3), University of British Columbia, Vancouver, Canada.

Cheung WWL, Close C, Kearney K, Lam V, Sarmiento J, Watson R, Pauly D (2009) Projections of global marine biodiversity impacts under climate change scenarios. *Fish and Fisheries* 10, 235–251.

Cheung WWL, Dunne J, Sarmiento JL, Pauly D (2011) Integrating ecophysiology and plankton dynamics into projected maximum fisheries catch potential under climate change in the Northeast Atlantic. *ICES Journal of Marine Science* 68 (6), 1008-1018.

Cheung WWL, Sarmiento JL, Dunne J, Frölicher T, Lam V, Palomares MLD, Watson R, Pauly D (2013). Shrinking of fishes exacerbates impacts of global ocean changes on marine ecosystems. *Nature Climate Change* 3, 254-258.

Close C, Cheung WWL, Hodgson S, Lam V, Watson R, Pauly D (2006) Distribution ranges of commercial fishes and invertebrates. In: Palomares, M. L. D., Stergiou, K. I., Pauly, D. (eds). Fishes in Databases and Ecosystems. Fisheries Centre Research Reports 14 (4). Fisheries Centre, University of British Columbia, Vancouver, p 27-37.

Delworth TL, Rosati A, Stouffer RJ, *et al.* (2006) GFDL's CM2 global coupled climate models. part I: formulation and simulation characteristics. *Journal of Climate* 19, 643-674.

Dickie LM, Kerr SR, Boudreau PR (1987) Size-dependent processes underlying regularities in ecosystem structure. *Ecological Monographs* 57, 233-250.

Dougherty J, Kohavi R, Sahami M (1995) Supervised and unsupervised discretization of continuous features. In: A. Prieditis and S. Russell, (eds.), Proceedings of International Conference on Machine Learning. Morgan Kaufmann, San Francisco, CA, USA, pp. 194-202.

Dulvy NK, Rogers SI, Jennings S, *et al.* (2008) Climate change and deepening of the North Sea fish assemblage: a biotic indicator of warming seas. *Journal of Applied Ecology* 45, 1029–1039.

Dunne JP, Gnanadesikan A, Sarmiento JL, Slater RD (2010) Technical description of the prototype version (v0) of tracers of phytoplankton with allometric zooplankton (TOPAZ) ocean biogeochemical model as used in the Princeton IFMIP model. *Biogeosciences* 7 (Suppl.), 3593.

Fayyad U, Irani K(1993) Multi-interval discretization of continuous-valued attributes for classification learning. In: Proceedings of the Thirteenth International Joint Conference on Artificial Intelligence. pp. 1022-1027.

Fernandes JA, Irigoien X, Boyra G, Lozano JA, Inza I (2009) Optimizing the number of classes in automated zooplankton classification. *Journal of Plankton Research* 31 (1), 19-29.

Fernandes JA, Irigoien X, Goikoetxea N, Lozano JA, Inza I, Pérez A, Bode A (2010) Fish recruitment prediction, using robust supervised classification methods. *Ecological Modelling* 221 (2), 338-352.

Frank KT, Petrie B, Fisher JA, Leggett WC (2011) Transient dynamics of an altered large marine ecosystem. *Nature* 477 (7362), 86-89.

Froese R, Zeller D, Kleisner K, Pauly D (2012) What catch data can tell us about the status of global fisheries. *Marine biology* 159 (6), 1283-1292.

Garcia SM, Cochrane KL (2005) Ecosystem approach to fisheries: a review of implementation guidelines. *ICES Journal of Marine Science* 62, 311-318.

Hagle TM, Glen EM (1992) Goodness-of-fit measures for Probit and Logit. *American*

Journal of Political Science 36 (3), 762-784.

Henson SA, Sarmiento JL, Dunne JP, *et al.* (2010) Detection of anthropogenic climate change in satellite records of ocean chlorophyll and productivity. *Biogeosciences* 7, 621-640.

Holt J, Butenschön M, Wakelin SL, Artioli Y, Allen JI (2012) Oceanic controls on the primary production of the northwest European continental shelf: model experiments under recent past conditions and a potential future scenario. *Biogeosciences* 9 (1), 97-117.

IPCC (2007) Summary for policymakers. In Climate Change 2007: the Physical Science Basis. Working Group I Contribution to the Fourth Assessment Report of the IPCC, pp. 1–18. Ed. by S. Solomon, D., Qin, M., Manning, Z., Chen, M., Marquis, K. B., *et al.* Cambridge University Press, Cambridge.

Jennings S, Mackinson S (2003) Abundance- body mass relationships in size structured food webs. *Ecology Letters* 6, 971-974.

Jennings S, Mélin F, Blanchard JL, Forster RM, Dulvy NK, Wilson RW (2008) Global-scale predictions of community and ecosystem properties from simple ecological theory. *Proceedings of the Royal Society B: Biological Sciences* 275 (1641), 1375-1383.

Jones MC, Dye SR, Fernandes JA, Frölicher TL, Pinnegar JK, Warren R, Cheung WWL (2013) Predicting the Impact of Climate Change on Threatened Species in UK Waters. PloS one, 8 (1), e54216.

Jones MC, Dye SR, Pinnegar JK, *et al.* (2012) Modelling commercial fish distributions: Prediction and assessment using different approaches. *Ecological Modelling* 225, 133-145.

Krause-Jensen D, Markager S, Dalsgaard T (2012) Benthic and Pelagic Primary Production in Different Nutrient Regimes. *Estuaries and coasts* 35 (2), 527-545.

Lam VW, Cheung WWL, Swartz W, Sumaila UR (2012) Climate change impacts on fisheries in West Africa: implications for economic, food and nutritional security. *African Journal of Marine Science* 34 (1), 103-117.

Large W, Yeager S (2009) The global climatology of an interannually varying air-sea flux data set. *Climate Dynamics* 33, 341-364.

Metcalfe JD, Le Quesne WJF, Cheung WWL, Righton DA (2012) Conservation physiology for applied management of marine fish: perspectives on the role and value of telemetry. *Philosophical Transactions of the Royal Society B* 367, 1746-1756.

Merino G, Barange M, Blanchard JL, et al. (2012) Can marine fisheries and aquaculture meet fish demand from a growing human population in a changing climate? *Global Environmental Change* 22 (4), 795-806.

Pauly D, Hilborn R, Branch TA (2013) Fisheries: Does catch reflect abundance? *Nature* 494 (7437), 303-306.

Pearson RG, Dawson TP (2003) Predicting the impacts of climate change on the distribution of species: are bioclimate envelope models useful? *Global Ecology and Biogeography* 12, 361-371.

Perry AL, Low PJ, Ellis JR, Reynolds JD (2005) Climate change and distribution shifts in marine fishes. *Science* 308, 1912-1915.

Perry RI, Ommer RE, Barange M, Jentoft S, Neis B, Sumaila UR (2011) Marine social–ecological responses to environmental change and the impacts of globalization. *Fish and Fisheries* 12 (4), 427-450.

Pörtner HO (2010) Oxygen- and capacity-limitation of thermal tolerance: a matrix for integrating climate-related stressor effects in marine ecosystems. *Journal of Experimental Biology* 213, 881-893.

Petitgas P, Alheit J, Peck MA, *et al.* (2012) Anchovy population expansion in the North Sea. *Marine Ecology-progress Series* 444, 1-13.

Ricard D, Minto C, Jensen OP, Baum JK (2012) Evaluating the knowledge base and status of commercially exploited marine species with the RAM Legacy Stock Assessment Database. *Fish and Fisheries* 13 (4), 380-398.

Rice J (2011), Managing fisheries well: delivering the promises of an ecosystem approach. *Fish and Fisheries* 12, 209-231.

Roessig JM, Woodley CM, Cech JJ, Hansen LJ (2004) Effects of global climate change on marine and estuarine fishes and fisheries. *Reviews in Fish Biology and Fisheries* 14, 251-275.

Schaefer MB (1954) Some aspects of the dynamics of populations important to the management of the commercial marine fisheries. *Bulletin of the Inter-American Tropical Tuna Commission* 1, 25-56.

Sheldon RW, Sutcliffe WH, Paranjape MA (1977) Structure of pelagic food chain and relationship between plankton and fish production. *Journal of the Fisheries Research Board of Canada* 34, 2344-2355.

Simpson SD, Jennings S, Johnson MP, Blanchard JL, Schön PJ, Sims DW, Genner MJ (2011) Continental shelf-wide response of a fish assemblage to rapid warming of the sea. *Current Biology* 21 (18), 1565-1570.

Steinacher M, Joos F, Frölicher TL, Bopp L, Cadule P, Doney SC, Gehlen M, Schneider B, Segschneider J (2010) Projected 21st century decrease in marine productivity: a multi-model analysis. *Biogeosciences* 7, 979-1005.

Stock CA, Alexander MA, Bond NA, *et al.* (2011) On the use of IPCC-class models to assess the impact of climate on living marine resources. *Progress in Oceanography* 88 (1-4), 1-27.

Taylor JR (1999) An introduction to error analysis: The Study of Uncertainties in Physical Measurements. University Science Books. pp. 128–129

Uusitalo L (2007) Advantages and challenges of Bayesian networks in environmental modelling. *Ecological Modelling* 203, 312-318.

Tables

Table 1. List of modelled fish species. Stocks that have been aggregated to provide species abundance estimates are identified by their stock ID codes (STOCKID) in the RAM Legacy database (upper case codes). For some ICES assessed stocks not listed in the RAM Legacy database, stock ID codes that were based on ICES Stock Summary Database were used (lower case codes).

Common name	Scientific name	Type	Stock ID code
Albacore	*Thunnus alalunga*	Pelagic	ALBANATL.
American plaice/long rough dab	*Hippoglossoides platessoides*	Demersal	
Angler	*Lophius piscatorius*	Demersal	
Atlantic cod	*Gadus morhua*	Demersal	CODNEAR, CODBA2224, CODBA2532, CODVIa, CODIS, CODICE, CODNS and CODKAT.
Atlantic herring	*Clupea harengus*	Pelagic	HERRIsum, HERRNS, HERR2224IIIa, HERR2532, HERR30, HERRRIGA, HERRNIRS, HERRNWATLC, HERR4VWX, HERR4RFA, HERR4RSP, HERR4TFA, HERR4TSP, HERR31, her-noss, hervian and her-vasu.
Atlantic horse mackerel	*Trachurus trachurus*	Pelagic	hom-west.
Atlantic mackerel	*Scomber scombrus*	Pelagic	MACKNEICES.
Baltic sprat	*Sprattus sprattus*	Pelagic	SPRAT22-32.
Blue whiting	*Micromesistius poutassou*	Pelagic	whb-comb.
Boarfish	*Capros aper*	Demersal	
Capelin	*Mallotus villosus*	Pelagic	CAPEICE and CAPENOR.
Common sole	*Solea solea*	Demersal	SOLENS, SOLEVIId, SOLEIS, SOLEIIIa, SOLEVIIe, SOLECS, and SOLEVIII.
Cuckoo ray	*Leucoraja naevus*	Demersal	
Dab	*Limanda limanda*	Demersal	
European anchovy	*Engraulis encrasicolus*	Pelagic	ANCHOBAYB.
European hake	*Merluccius merluccius*	Demersal	HAKESOTH and HAKENRTN.
European pilchard	*Sardina pilchardus*	Pelagic	sar-soth.
European plaice	*Pleuronectes platessus*	Demersal	PLAIC7d, PLAICIIIa, PLAICNS, PLAICIS, PLAICECHW and PLAICCELT.
European sprat	*Sprattus sprattus*	Pelagic	SPRATNS.
Flounder	*Platichthys flesus*	Demersal	
Fourbeard rockling	*Enchelyopus cimbrius*	Demersal	
Fourspotted megrim	*Lepidorhombus boscii*	Demersal	mgb-8c9a.

Greenland halibut	*Reinhardtius hippoglossoides*	Demersal	GHALNEAR, GHALBSAI and GHAL23KLMNO.
Haddock	*Melanogrammus aeglefinus*	Demersal	HAD4X5Y, HAD5Y, HAD5Zejm, HADICE, HADNEAR, HADFAPL, HADNS-IIIa, HADVIa, HADVIIb-k, HADROCK and HADGB.
John dory	*Zeus faber*	Demersal	
Lemon sole	*Microstomus kitt*	Demersal	
Ling	*Molva molva*	Demersal	
Megrim	*Lepidorhombus whiffiagonis*	Demersal	mgw-8c9a.
Northern bluefin tuna	*Thunnus thynnus*	Pelagic	ATBTUNAEATL and ATBTUNAWATL.
Norway pout	*Trisopterus esmarkii*	Demersal	nop-34.
Golden Redfish	*Sebastes norvegicus*	Demersal	GOLDREDNEAR.
Pearlsides	*Maurolicus muelleri*	Pelagic	
Piked dogfish/ Spurdog	*Squalus acanthias*	Demersal	
Pollack	*Pollachius pollachius*	Demersal	
Poor cod	*Trisopterus minutus*	Demersal	
Pouting / Bib	*Trisopterus luscus*	Demersal	
Red bandfish	*Cepola macrophthalma*	Demersal	
Saithe / Pollock	*Pollachius virens*	Demersal	POLL5YZ, POLLNEAR, POLLFAPL, POLL4X5YZ and POLLNS-VI-IIIa.
Smallspottedcatshark	*Scyliorhinus canicula*	Demersal	
Splendid alfonsino	*Beryx splendens*	Demersal	
Spotted ray	*Raja montagui*	Demersal	
Striped red mullet	*Mullus surmuletus*	Demersal	
Thickback sole	*Microchirus variegatus*	Demersal	
Thornback ray	*Raja clavata*	Demersal	
Tub gurnard	*Chelidonichthys lucerna*	Demersal	
Tusk/ Torsk / Cusk	*Brosme brosme*	Demersal	CUSK4X.
Whiting	*Merlangius merlangus*	Demersal	WHITNS-VIId-IIIa, WHITVIa and WHITVIIek.
Witch	*Glyptocephalus cynoglossus*	Demersal	

Table 2. Summary of abbreviations.

Abbreviation	Description	Details
DBEM	Dynamic Bioclimate Envelope Model	
$E\_C_{Spp,W,i}^{Suit}$	Biomass by competition	$res_{Spp,W,i}^{Suit} \cdot E\_S$
$E\_D_{Spp,W,i}^{Suit}$	Biomass demanded	Calculated at each yearly shift
ERSEM	European Regional Seas Ecosystem Model	
$E\_S_{size,i}$	Total biomass supported in a cell	Calculated from Primary production
GFDL	Geophysical Fluid Dynamic Laboratory Earth	System model
I	Index of cell	From 0 to 250200
NSI	No species interactions	
$res_{Spp,W,i}^{Suit}$	Actual proportion of resources by competition	See Fig. 2
$res_{Spp,Suit,W}$	Proportion resources at matrix of energy demand	See Eq. 4
$Res\_op_{Spp,Suit,W}$	Proportion of resources by opportunity	See Eq. 6
Spp	Index of species	From 0 to 48 species
SS	Size-spectrum (based interactions)	
Suit	Index of the habitat suitability bin	Between 0 and 4 bins
$TotalRes_{W,i}$	Total proportion of resources demanded	$\sum_{Spp} res_{Spp,W,i}^{Suit}$
W	Index of the size spectrum	21 $\log_2$ classes from 2^{-1} to 2^{19}

Table 3. Average latitudinal shift in different simulations. NSI corresponds to simulations where the model does not incorporate species interactions through the size-spectrum, whereas SS denotes the use of the species interactions algorithm. GFDL and ERSEM correspond to two different Earth System Models.

	Latitudinal Shift (km decade^{-1})		
Projection	All species	Demersal	Pelagic
NSI-DBEM GFDL	16.7	14.1	26.0
SS-DBEM GFDL	13.7	12.6	18.4
NSI-DBEM ERSEM	18.1	15.2	28.2
SS-DBEM ERSEM	15.7	15.3	16.9

Figures:
Fig. 1: Relationship between the maximum assessed biomass (log) and the estimated carrying capacity of fish population (B_∞, log) for 22 species in the 27 FAO area (after removing extreme values, the lowest and highest B_∞).

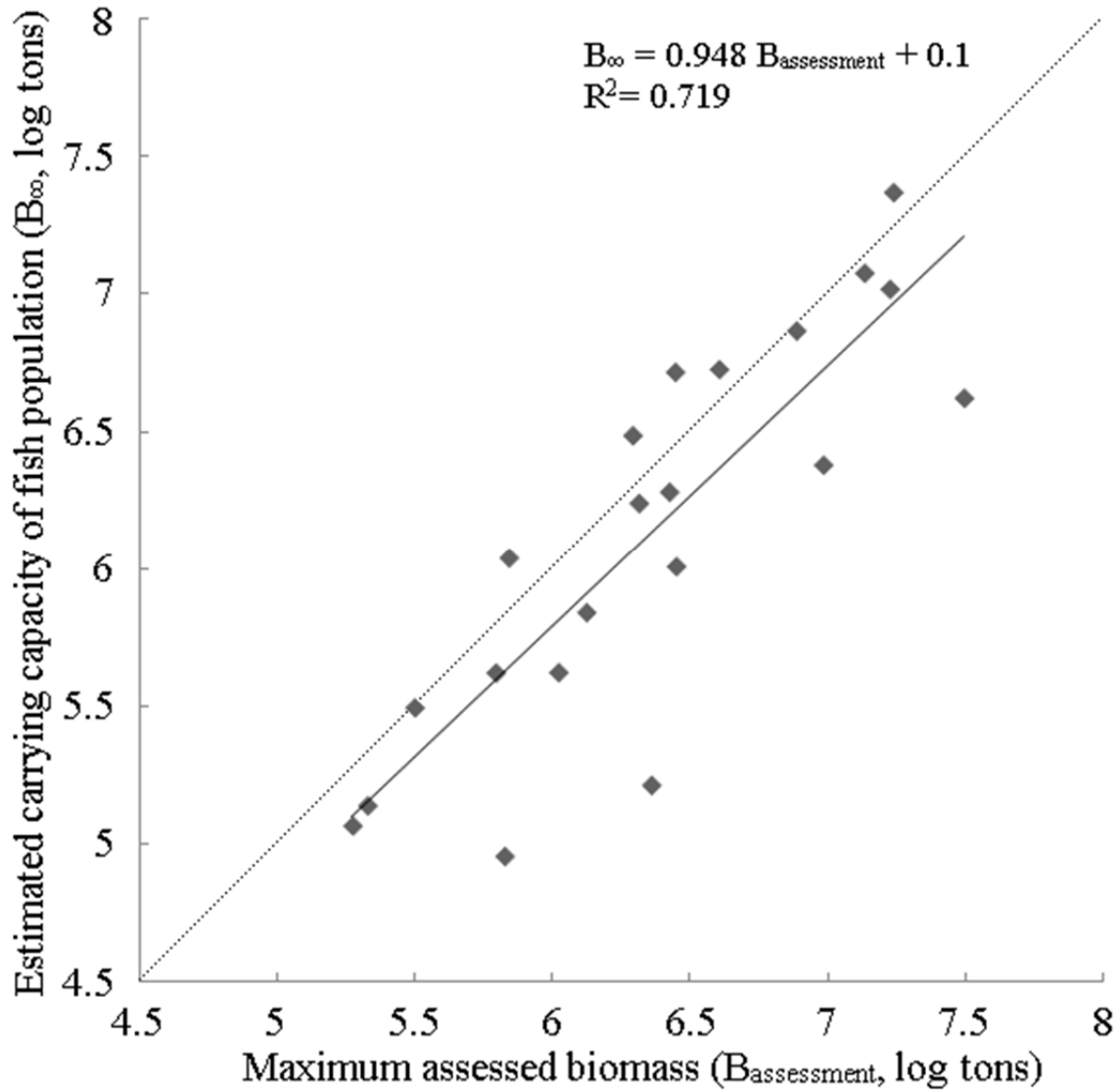$B_\infty = 0.948\ B_{assessment} + 0.1$
$R^2 = 0.719$

Fig. 2: Framework to calculate the matrix of energy demand at each size class for each species and to calculate the effects of species interactions.

ICES Stock Summary database
Ram Legacy Stock Assessment database

Species initial biomass

SeaAroundUsBase
FishBase

Taxa parameters | Species distribution

Temperature
Advection
Salinity
Other

Earth system models
ERSEM, GFDL, ...

Primary production
Temperature

Size spectrum model
Jennings et al., 2008

Dynamic bioclimate envelop model
Cheung et al., 2008; 2009; 2011

LINK BETWEEN MODELS
Species interactions table

Biomass supported at each size bin

Size distribution for each species

Algorithm for species interactions

Size distribution for each species

Initial biomass

Relative distribution across cells

Size distribution

Total biomass supported at each size bin in each cell

% resources demanded at each size bin

Habitat suitability in each cell

Species interactions table for each species: i.e. % resources demanded at each size bin by habitat suitability

Algorithm pseudocode for species interactions

1: Calculate $E\_C^{Suit}_{Spp,W,i} = res_{Spp,Suit,W} * E\_S$

2: If $E\_C^{Suit}_{Spp,W,i} > E\_D^{Suit}_{Spp,W,i}$ then % $res^{Suit}_{Spp,Size,i} = E\_D^{Suit}_{Spp,W,i} / E\_S_{W,i}$

3: $TotalRes_{W,i} = \sum_{Spp} res^{Suit}_{Spp,W,i}$

4: If $TotalRes_{W,i} < 1$ then $res^{Suit}_{PP,W,i} = Res\_op_{Spp,Suit,W} \cdot Res\_op_{Spp,Suit,W}$

5: If $TotalRes_{W,i} > 1$ then Normalize: $res^{Suit}_{Spp,W,i} = res^{Suit}_{Spp,W,i} / TotalRes_{W,i}$

6: If $res^{Suit}_{Spp,W,i} > Res\_op_{Spp,Suit,W}$ then $res^{Suit}_{Spp,W,i} = Res\_op_{Spp,Suit,W}$

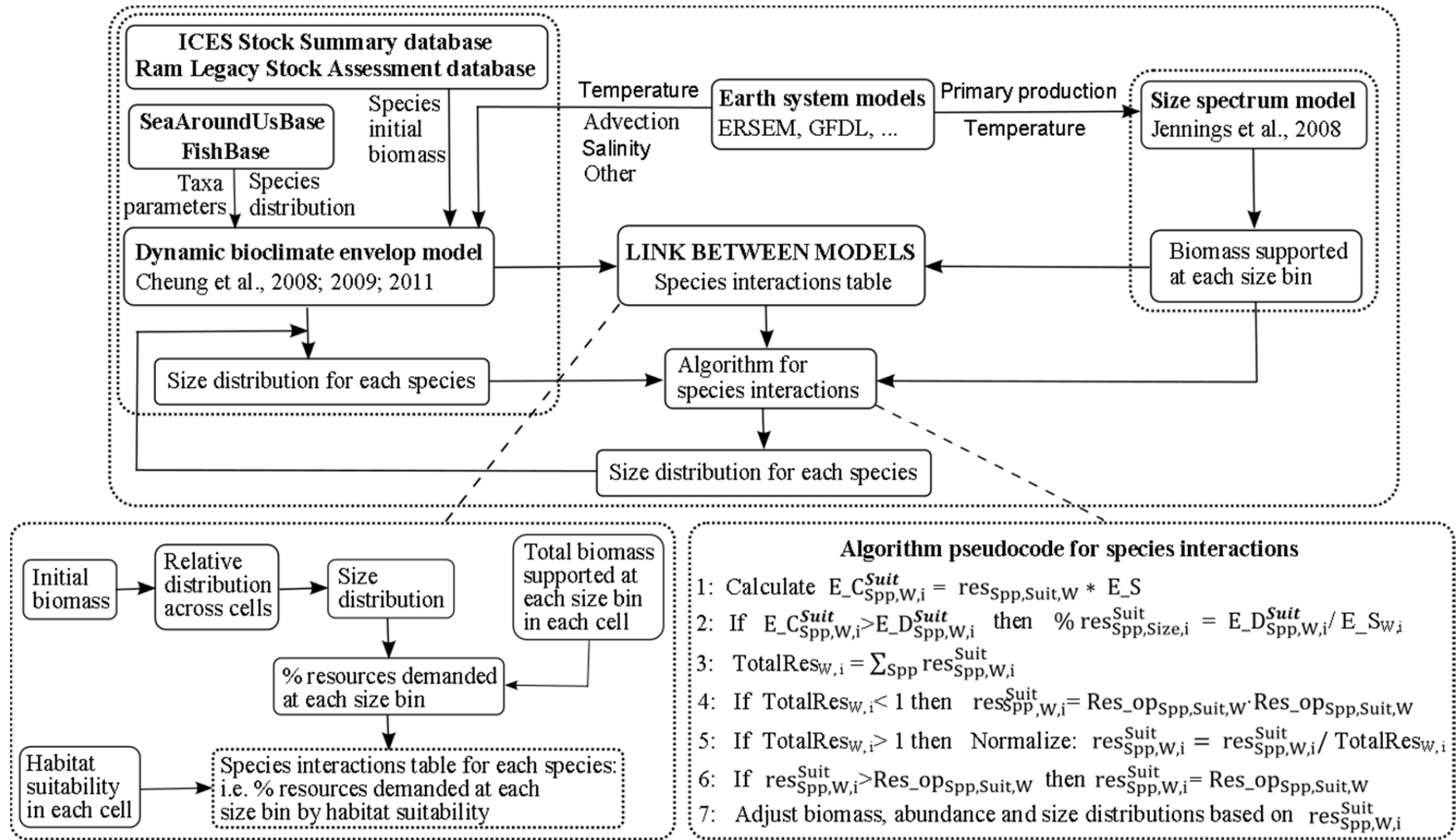7: Adjust biomass, abundance and size distributions based on $res^{Suit}_{Spp,W,i}$

Fig. 3: Species biomass by body mass class supported in a single coastal cell (30' x 30'), used as an example. Open circles represent the biomass that can be supported in this cell using only the size-spectrum component of the model.
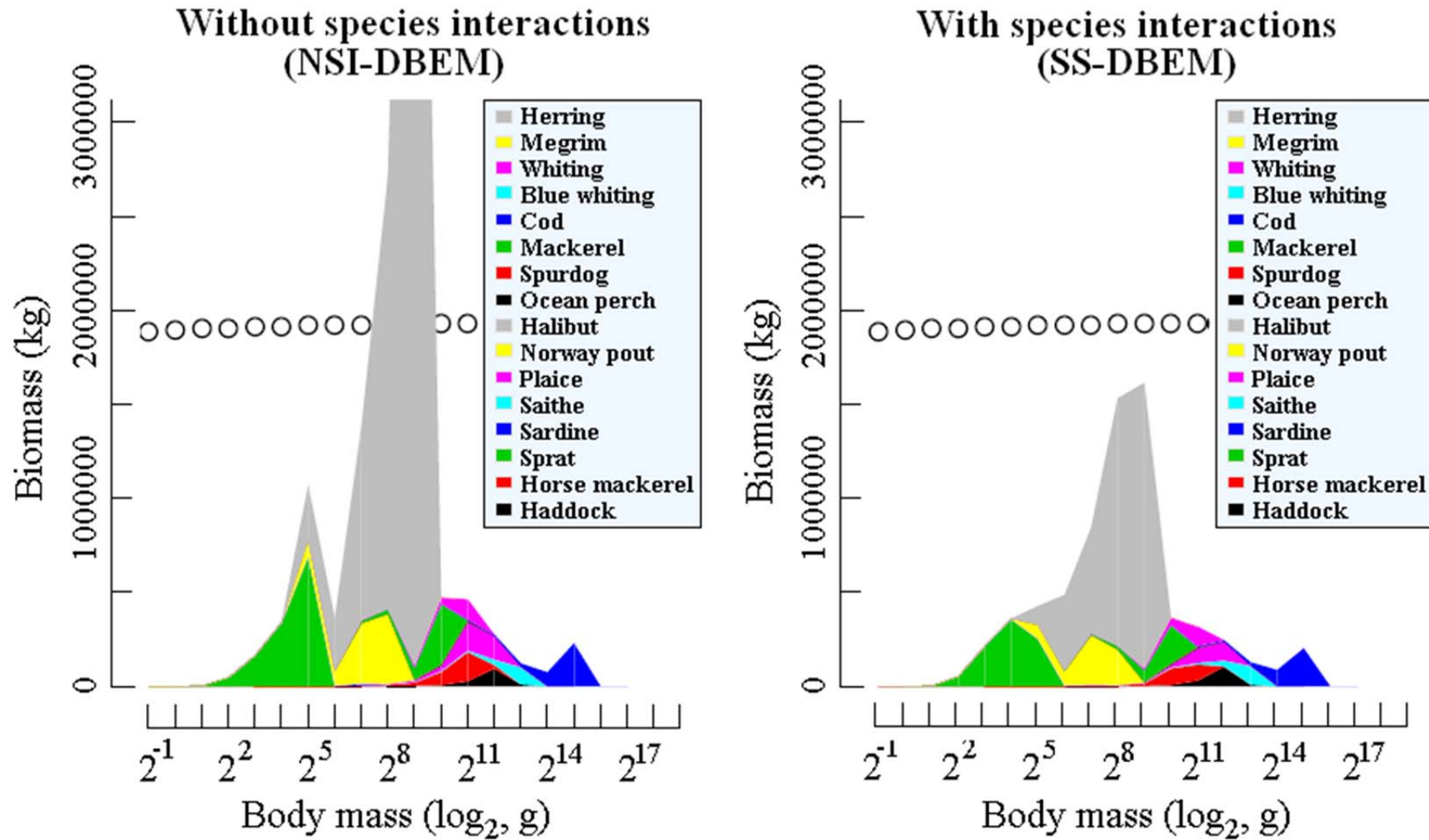
Fig. 4: Distribution of absolute error of predicted biomass for SS-DBEM and NSI-DBEM and the biomass estimated from stock assessments for the 1991 to 2003 period in the Northeast Atlantic (FAO Area 27). The time-series have been normalized between 0 and 1 before calculating the absolute error, to ensure that species' absolute abundances do not affect the results. The comparison is presented for ERSEM (left) and GFDL (right) showing in the legend mean and standard deviation of the absolute error. A narrower distribution of error (lower standard deviation) in SS-DBEM is indicative of a higher precision.
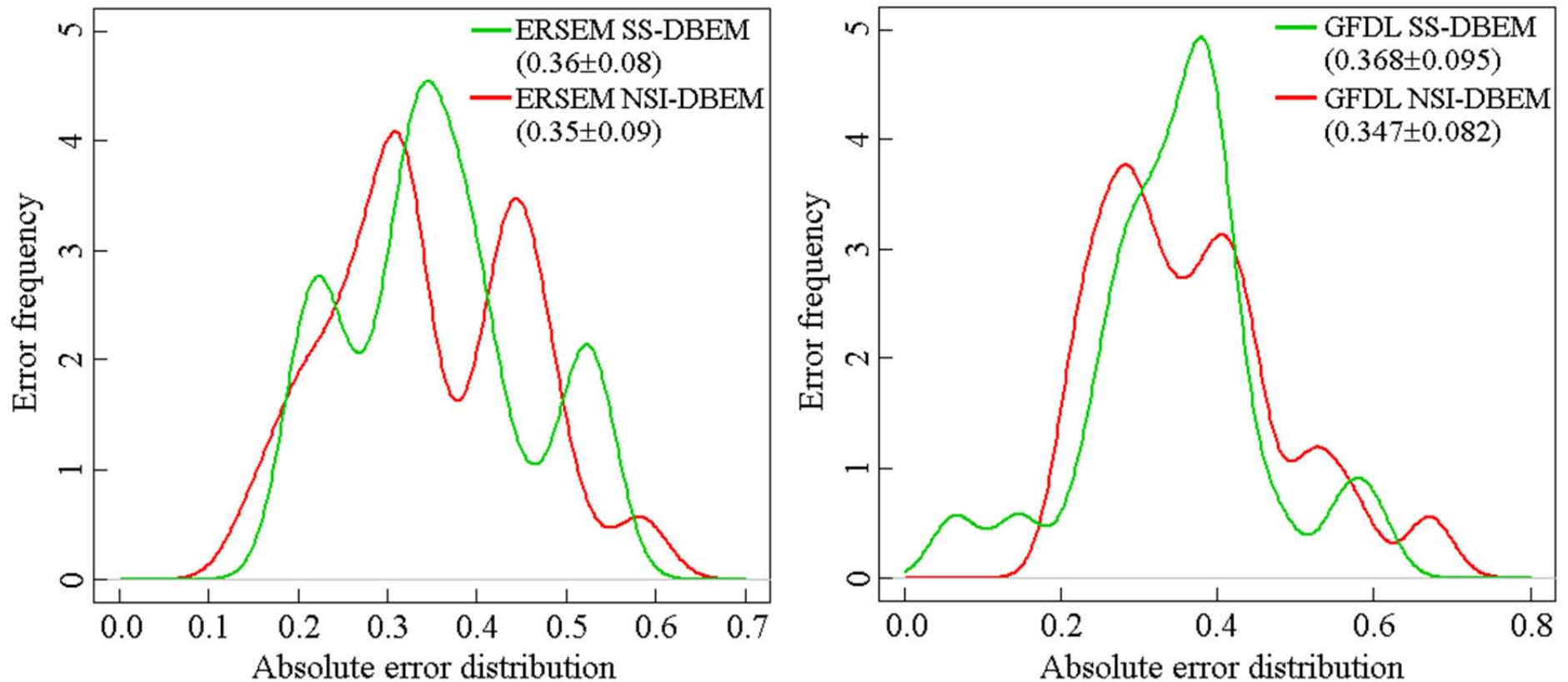
Fig. 5: Predicted latitudinal shift of distribution centroids of 49 species of fishes from 1971 to 2004 using ERSEM climatic dataset for the NSI-DBEM and SS-DBEM. The thick dark bar represents the median shift of all the species in a year, the lower and upper boundaries of the box represent the 25% and 75% quartiles, respectively. Positive value indicates poleward shift relative to species distribution in 1971.
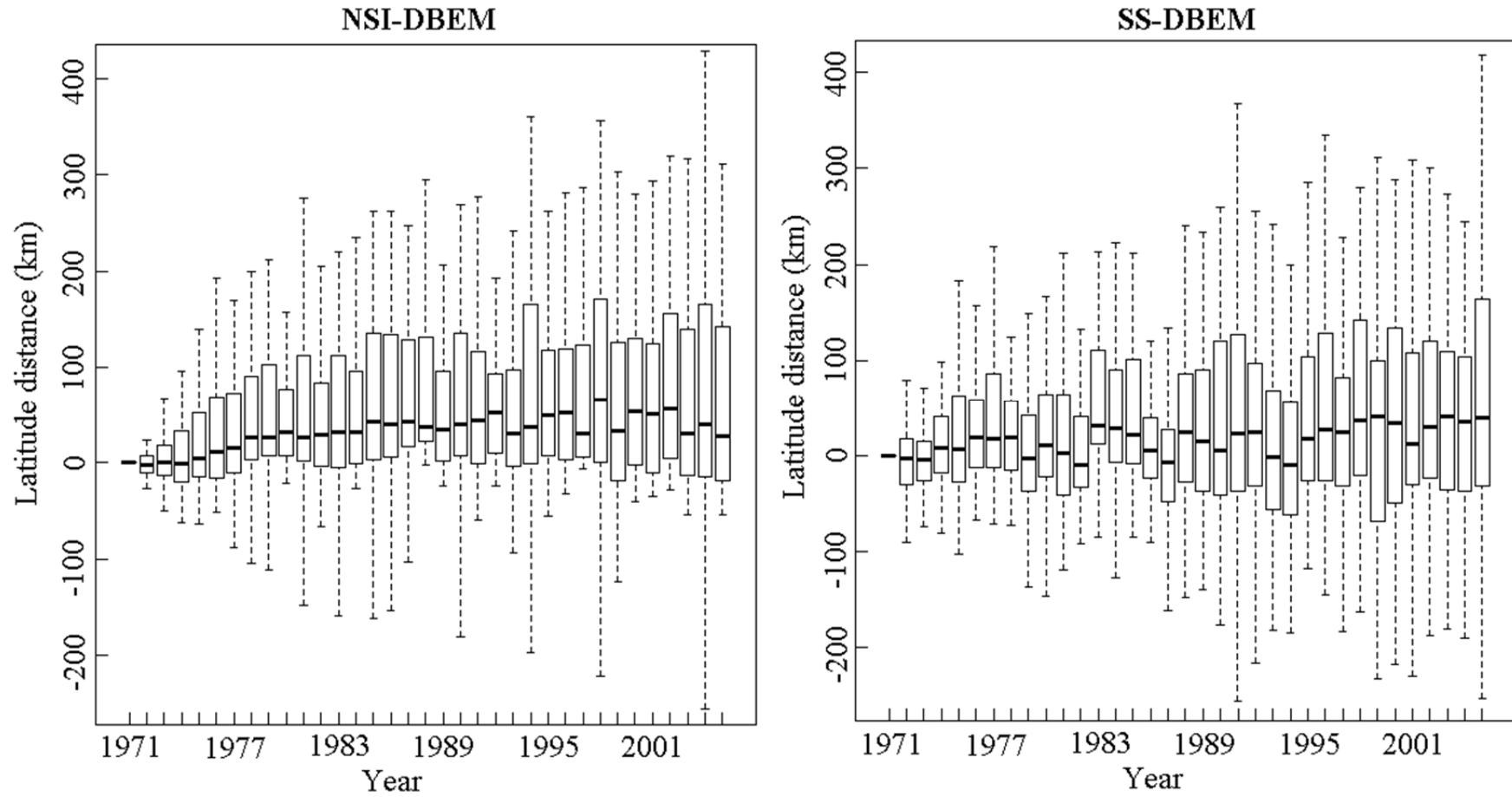
Fig. 6: Predicted changes in maximum catch compared with empirical catch data. Time-series has been normalized between 0 and 1 in order to compare inter-annual variability.